



Chapter 23

Development of a New Normalization Technique for Twelve Fringe Photoelasticity (TFP)

Ashutosh Pandey and K. Ramesh

Abstract The use of theoretical calibration table for fringe pattern demodulation in isochromatic images is revisited and a sensitivity analysis of material stress fringe value to generate theoretical calibration table is studied. The influence of filter parameter 'R' in normalization is discussed and its nuances are brought out. A substitution for theoretical calibration table and a new normalization technique is proposed to alter the dynamic range over the entire model domain of the isochromatic image suitably.

Keywords Photoelasticity · Fringe pattern analysis · Theoretical calibration · Image processing · Normalization

23.1 Introduction

In TFP/RGB photoelasticity, isochromatic images recorded in white light are generally demodulated to get fringe order by using experimental calibration table [1]. Recently fringe demodulation has been explored by the use of fringe pattern normalization [2] in conjunction with theoretically generated calibration table (CT) [3]. To generate the theoretical CT, the procedure demands accurate evaluation of material stress fringe value (F_σ) for each of the channels. However, no sensitivity analysis has been reported in the literature. In this paper, the sensitivity of F_σ (N/mm/fringe-order) values of red and blue channels for theoretical CT is studied. One of the first steps in new fringe demodulation approach is that isochromatic image needs to be normalized. The normalization uses a frequency filter's parameter 'R' to change the dynamic range in the image. The choice of 'R' plays an important role in normalization and its influence for a standard problem of circular disc under diametral compression is brought out. A new normalization technique is proposed and a study of fringe order demodulation in circular disc under diametral compression with a normalized experimental calibration table is done and the results are compared with corresponding analytical solution.

23.2 Sensitivity Analysis of Theoretical Calibration Table

An isochromatic image of an epoxy C-specimen having $F_{\sigma\text{-red}} = 13.174$, $F_{\sigma\text{-green}} = 11.62$ and $F_{\sigma\text{-blue}} = 9.15$ is recorded till 12th fringe order (N) and a section till fourth fringe order is shown in Fig. 23.1a, which is normalized with $R = 5$ and is shown in Fig. 23.1b. Theoretical CT is generated with same F_σ values as application specimen (CT-1) and is shown in Fig. 23.1c. Since these F_σ values are experimentally calculated, there is a possibility of error in calculating F_σ . To study the effect of small errors in F_σ calculation on fringe order demodulation, an error of -2.5% in blue channel and $+2.5\%$ in red channel is introduced to generate a CT-2 which is shown in Fig. 23.1d. Intensity representation of the difference in grey values between CT-1 and CT-2 is shown in Fig. 23.1e. The plot of grey values along line AB is shown in Fig. 23.1f. Fringe order in normalized image (Fig. 23.1b) is demodulated by CT-1 and CT-2, the corresponding colour representation is shown in Fig. 23.1g, h respectively. The plot of difference of N_{CT} along line AB in Fig. 23.1g and 1 h with $N_{analytical}$ is shown in Fig. 23.1i which shows that the mean absolute deviation (MAD) of difference in fringe order by CT-2 is 0.14 which is 3.5 times greater than the MAD of 0.04 by CT-1.

A. Pandey · K. Ramesh (✉)
Department of Applied Mechanics, Indian Institute of Technology Madras, Chennai, India
e-mail: kramesh@iitm.ac.in

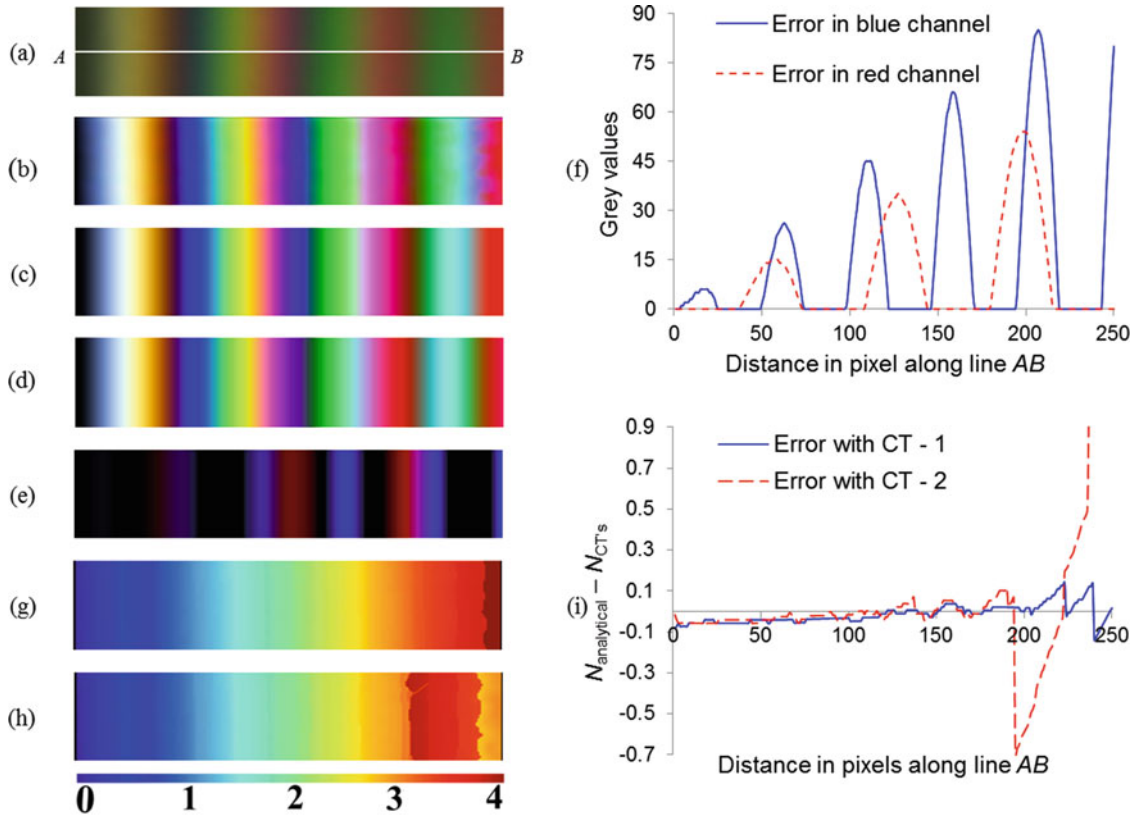


Fig. 23.1 (a) Cropped isochromatic image of epoxy C-specimen up to fourth fringe order, (b) Epoxy C-specimen image in 'a' normalized with $R = 5$, Intensity representation of theoretical calibration table: (c) with actual F_{σ} values (CT-1) (d) with error in red and blue channel F_{σ} values (CT-2), (e) Intensity representation of difference in grey scale values between CT-1 and CT-2, (f) Plot of grey values along line AB in 'e', Colour map of fringe order (N) by: (g) CT-1 (h) CT-2, (i) Error plot of fringe order by CT-1 and CT-2 with analytical solution along line AB

23.3 Influence of Filter Radius on Normalization and New Normalization Technique

In normalization, Phani et al. [4] demonstrated that a single R is insufficient to remap dynamic range in low and high fringe gradient zones. An epoxy circular disc (Fig. 23.2a) recorded with a load of 492 N , when normalized with $R = 2$, a loss of intensity values is seen at high fringe gradient zones (Fig. 23.2b) and when normalized with $R = 30$, noise intensities come at low fringe gradient zones (Fig. 23.2c). To handle this issue, a new normalization technique is proposed which uses a high pass (H_{HP}) and low pass (H_{LP}) filter, which are defined as follows:

$$H_{HP} = 1 - e^{\left(\frac{\sqrt{(u^2+v^2)}}{2R_1^2}\right)}, \text{ where } R_1 \text{ is the radius of the } H_{HP} \quad (23.1)$$

$$H_{LP} = e^{\left(-\frac{\sqrt{(u^2+v^2)}}{2R_2^2}\right)}, \text{ where } R_2 \text{ is the radius of the } H_{LP} \quad (23.2)$$

where u and v are the matrices defined for an isochromatic image of size $m \times n$ as follows. where R is the radius of the frequency filter, u and v are the matrices defined as

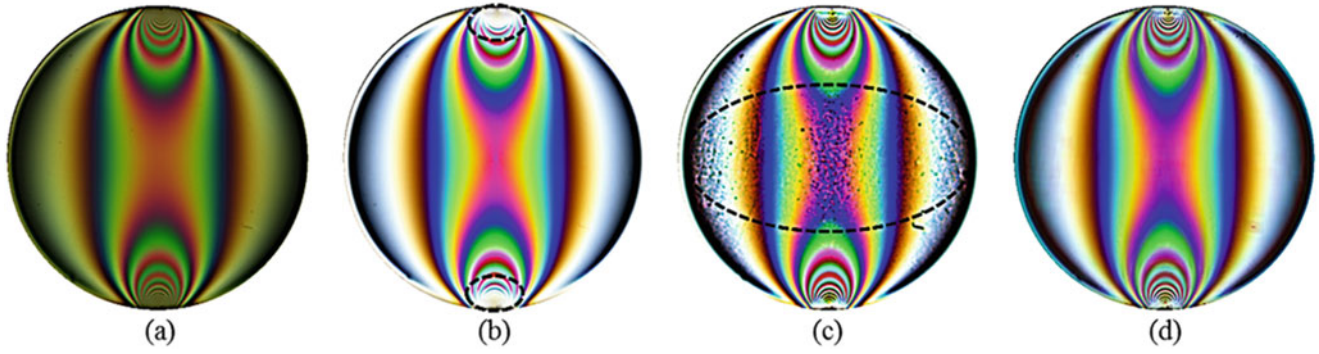


Fig. 23.2 (a) Isochromatic image of a circular disc with a load of 492 N, Image 'a' normalized with: (b) $R = 2$ (c) $R = 30$, (d) $R_1 = 30$ and $R_2 = 10$

$$u = \begin{bmatrix} 1 - u_0 & 2 - u_0 & \dots & n - u_0 \\ 1 - u_0 & 2 - u_0 & \dots & n - u_0 \\ \dots & \dots & \dots & \dots \\ 1 - u_0 & 2 - u_0 & \dots & n - u_0 \end{bmatrix}_{m \times n} \quad v = \begin{bmatrix} 1 - v_0 & 1 - v_0 & \dots & 1 - v_0 \\ 2 - v_0 & 2 - v_0 & \dots & 2 - v_0 \\ \dots & \dots & \dots & \dots \\ m - v_0 & m - v_0 & \dots & m - v_0 \end{bmatrix}_{m \times n}, \quad \text{where } u_0 = \frac{n}{2} + 1 \text{ and } v_0 = \frac{m}{2} + 1 \quad (23.3)$$

The circular disc in Fig. 23.2a is normalized with filter's radius $R_1 = 30$ and $R_2 = 10$ and shown in Fig. 23.2d, which clearly demonstrates that this algorithm has an ability to alter the dynamic range over the complete image reasonably better.

23.4 Whole-Field Fringe Order Evaluation with Normalized Experimental Calibration Table

An isochromatic image of circular disc (Fig. 23.3a) having diametral compression of 1373 N and $F_\sigma = 10.4$ N/mm/fringe-order for a wavelength of 546.1 nm is normalized with $R_1 = 30$ and $R_2 = 10$ and is shown in Fig. 23.3b. The calibration table is generated by normalizing the same epoxy isochromatic specimen (normalized CT) in Fig. 23.1a till 16th fringe order with $R_1 = 30$ and $R_2 = 10$. The colour map of fringe order obtained by using normalized CT is shown in Fig. 23.3c. The colour map of absolute error between fringe order in Fig. 23.3c and analytical fringe orders is shown in Fig. 23.3d. The plot of fringe order along lines CD and EF (Fig. 23.3e) shows a close match with analytical results.

23.5 Conclusion

The study of small changes in material stress fringe value shows that the theoretical calibration table is highly sensitive to this. Normalization algorithm is influenced by filter parameter ' R ' and a single value of ' R ' is not sufficient to alter the dynamic range in the image. The new normalization technique is capable of alter the dynamic range over the complete domain of the isochromatic image reasonably better. Use of experimentally recorded calibration table after normalization is found to extract up to 16th fringe orders.

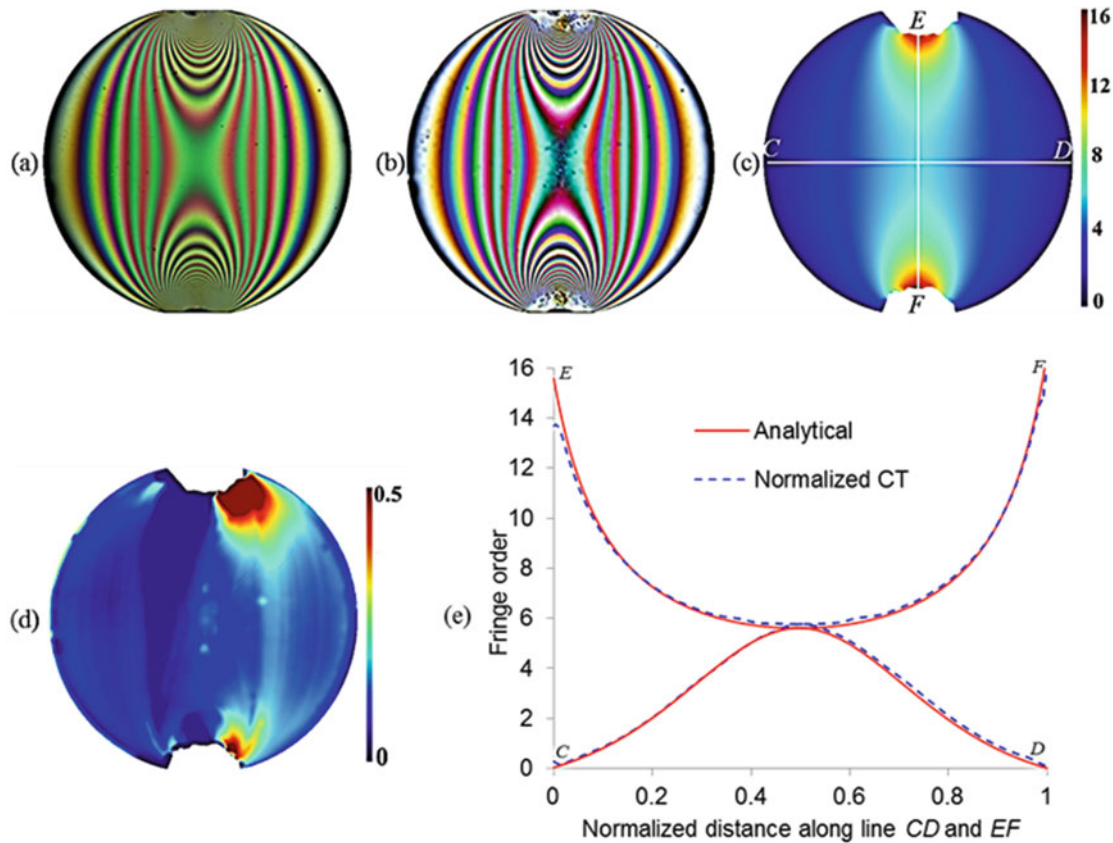


Fig. 23.3 (a) Isochromatic image of a circular disc with a load of 1373 N, (b) Image 'a' normalized with $R_1 = 30$ and $R_2 = 10$, (c) Colour map of fringe order obtained using normalized CT, (d) Colour map of absolute error between 'c' and analytical fringe orders, (e) The plot of fringe orders along line CD and EF in 'c'

References

1. Ramesh, K.: Digital photoelasticity. In: Rastogi, P. (ed.) *Digital Optical Measurement Techniques and Applications*, pp. 289–340. Artech House, Norwood MA (2015)
2. Larkin, K.G., Bone, D.J., Oldfield, M.A.: Natural demodulation of two-dimensional fringe patterns. I. General background of the spiral phase quadrature transform. *J. Opt. Soc. Am. A.* **18**(8), 1862–1870 (2001)
3. Swain, D., Thomas, B.P., Philip, J., Pillai, S.A.: Non-uniqueness of the color adaptation techniques in RGB photoelasticity. *Exp. Mech.* **55**, 1031–1045 (2015)
4. Phani Madhavi, C., Ramakrishnan, V., Ramesh, K.: Critical assessment of fringe pattern normalization for twelve fringe photoelasticity. In: Yoshida, S., Lamberti, L., Sciammarella, C.A. (eds.) *Advancement of Optical Methods in Experimental Mechanics*, pp. 295–299. Springer, Berlin (2017)